JACS
JOURNAL OF THE AMERICAN CHEMICAL SOCIETY

ARTICLE

pubs.acs.org/JACS

Telomestatin: Formal Total Synthesis and Cation-Mediated Interaction of Its *seco*-Derivatives with G-Quadruplexes

Jörg Linder,[†] Thomas P. Garner,[†,‡] Huw E. L. Williams,[†,‡] Mark S. Searle,[†,‡] and Christopher J. Moody*[,†]

[†]School of Chemistry and [‡]Centre for Biomolecular Sciences, University of Nottingham, University Park, Nottingham NG7 2RD, United Kingdom

Supporting Information

ABSTRACT: The structurally unique natural product telomestatin incorporates seven oxazole rings and one sulfur- containing thiazoline in a macrocyclic arrangement. The compound is a potent inhibitor of the enzyme telomerase and therefore provides a structural framework for developing new potential therapeutic agents for cancer. An efficient formal total synthesis of telomestatin is reported in which the key steps are the use of dirhodium(II)-catalyzed reactions of diazocarbonyl compounds to generate six oxazole rings, demonstrating the power of rhodium carbene methodology in organic chemical synthesis. CD spectroscopy establishes that *seco*-derivatives of telomestatin are potent stabilizers of G-quadruplex structures derived from the human telomeric repeat sequence. Mass spectrometry studies, confirmed by molecular dynamics simulations, provide the first evidence that high affinity binding to terminal G-tetrads in both 1:1 and 2:1 ligand complexes is mediated through the macrocycle coordinating a monovalent cation, with selectivity for the antiparallel structure.

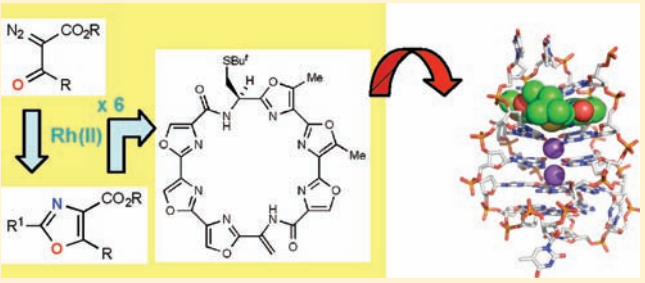

INTRODUCTION

Telomerase is a ribonucleoprotein with reverse transcriptase activity that serves to protect and maintain the length of telomeric DNA (the guanine-rich TTAGGG repeat sequences) at the ends of chromosomes during replication. While the shortening of DNA telomeres during repeated cell division is a natural part of the cellular aging mechanism, rapidly dividing cancer cells, on the other hand, have increased telomerase activity, thereby allowing them to maintain their telomere length. This maintenance of telomeres is a feature of almost all malignant cells, and hence telomerase has a key function in their limitless replicative potential (or immortality),[1] one of the six hallmarks of cancer.[2]

The discovery and unravelling of the fundamental role of telomerase was recently recognized by the award of the 2009 Nobel Prize for Physiology or Medicine to Blackburn, Greider, and Szostak. However, interfering with the mechanism of action of telomerase has also led to the possibility of new therapies based on its inhibition, because this should restore normal DNA replicative shortening by loss of telomeres, leading to normal aging and cell death. As a result, there has been substantial activity in trying to identify potent inhibitors of telomerase as potential anticancer agents.[3−6] The mechanism of action of telomerase is dependent upon both an endogenous RNA template and a single-stranded DNA primer for the effective addition of telomeric repeats.[7] However, G-rich telomeric sequences are able to self-assemble into four stranded G-quadruplex structures consisting of G-tetrads stabilized by monovalent cations (Figure 1).[8] Although the formation of compact folded quadruplex structures alone inhibits telomerase activity,[9] the search for quadruplex-specific ligands that further enhance the stability of the folded state has focused attention on the discovery of new anticancer agents that act at the DNA level.[3−6]

In the search for new medicinal agents, nature has often served as the inspiration; natural products have emerged via biosynthesis by proteins, and these evolutionary selected structures have the prerequisites for binding to proteins and penetrating cell membranes, and therefore they regularly provide new starting points for drug discovery programs.[10] Indeed, of the new therapies introduced for cancer treatment in the period January 1981 to mid-2008, almost 80% have their origins in natural products.[10] Hence, it is perhaps not surprising that one of the most potent inhibitors of telomerase discovered to date is a natural product, telomestatin **1**.[11] This compound, isolated from *Streptomyces anulatus*, possesses a unique structure incorporating one thiazoline (ring H) and seven oxazole rings (A−G) in a macrocyclic array and is a potent and specific inhibitor of telomerase (IC_{50} = 5 nM).[11] However, it was the observation by Hurley and co-workers that telomestatin structurally resembles a G-tetrad **2** (Figure 1)[12] and their subsequent demonstration that it selectively stabilizes the formation of the intramolecular G-quadruplex formed from the human telomeric

Received: October 12, 2010
Published: December 16, 2010

dx.doi.org/10.1021/ja109158k | *J. Am. Chem. Soc.* 2011, 133, 1044–1051

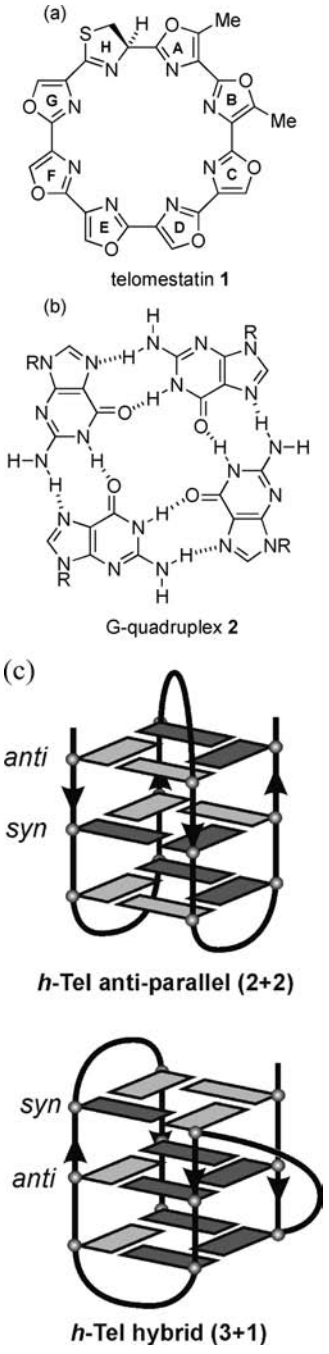

Figure 1. (a) Structure of the natural product telomestatin **1**; (b) structure of a G-tetrad **2** (R = deoxyribose sugar) (the tetrad is stabilized by a monovalent cation coordinated at the center of the G-tetrad, not shown); and (c) schematic representation of the proposed mixture of (2 + 2) antiparallel and hybrid (3 + 1) structures formed by the *h*-Tel sequence. The different glycosidic torsion angles (syn and anti) that allow these different structural topologies are highlighted.

TTAGGG repeat sequences that has stimulated much of the ensuing work with this fascinating natural product and related analogues.[13,14] More recent studies have also suggested a cellular mode of action of telomestatin and analogues, which results in a novel antiproliferative and apoptotic activity that is independent of telomerase, causing M-phase cell cycle arrest even in telomerase-negative cell lines.[15]

Scheme 1. Plan for the Synthesis of Telomestatin (R = Suitable Protecting Group)

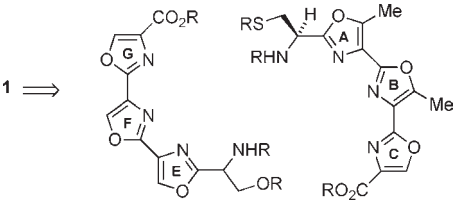

Scheme 2. Rhodium Carbene Routes to Oxazoles from Carboxamides

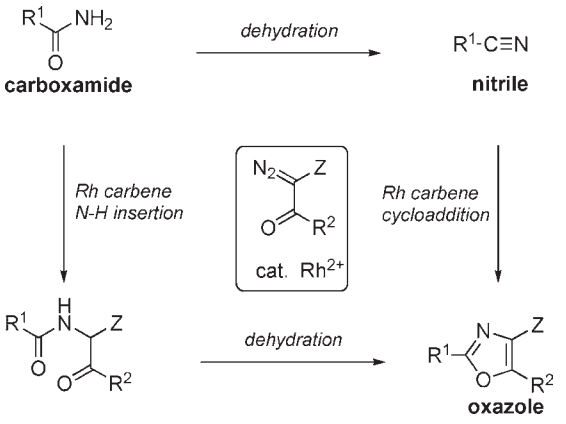

The unique hepta-oxazole structure of telomestatin has spawned a substantial amount of effort on the synthesis and G-quadruplex binding properties of a number of macrocycles containing three, four, six, or seven oxazole rings, either linked directly (as in telomestatin) or via amide bonds.[15−23] However, despite all this work on analogues, and the clear interest in the biological activity of telomestatin itself, to date there have been only two syntheses of the natural product reported, the first in a patent,[24,25] although a number of other approaches to poly oxazoles have been described.[26−33] Oxazole-containing natural products continue to capture the imagination of chemists, not only because of their structural diversity but also their biological activity, and therefore remain topical targets for synthesis. We now describe a formal total synthesis of telomestatin employing rhodium carbene chemistry to generate six oxazole rings, and the potent G-quadruplex stabilizing activity of its *seco*-derivatives. In addition, ESI-MS studies of these derivatives reveal that the macrocycle is readily able to coordinate monovalent cations (NH_4^+ and K^+) in the complex that facilitates stacking on the terminal G-tetrads in both 1:1 and 2:1 ligand complexes, the first evidence for the involvement of cations in the stabilization of the end-capping interaction with G-tetrads.

RESULTS AND DISCUSSION

Synthesis. The plan for the synthesis of telomestatin involved its disconnection into two tris-oxazoles, the right-hand fragment comprising rings A−C and the left fragment of rings E−G, their subsequent conjuncture, followed by formation of oxazole ring D, and thiazoline ring H (Scheme 1). Although the

dx.doi.org/10.1021/ja109158k |*J. Am. Chem. Soc.* 2011, 133, 1044–1051

Scheme 3. Synthesis of Right-hand Tris-oxazole Fragment (Rings A−C)

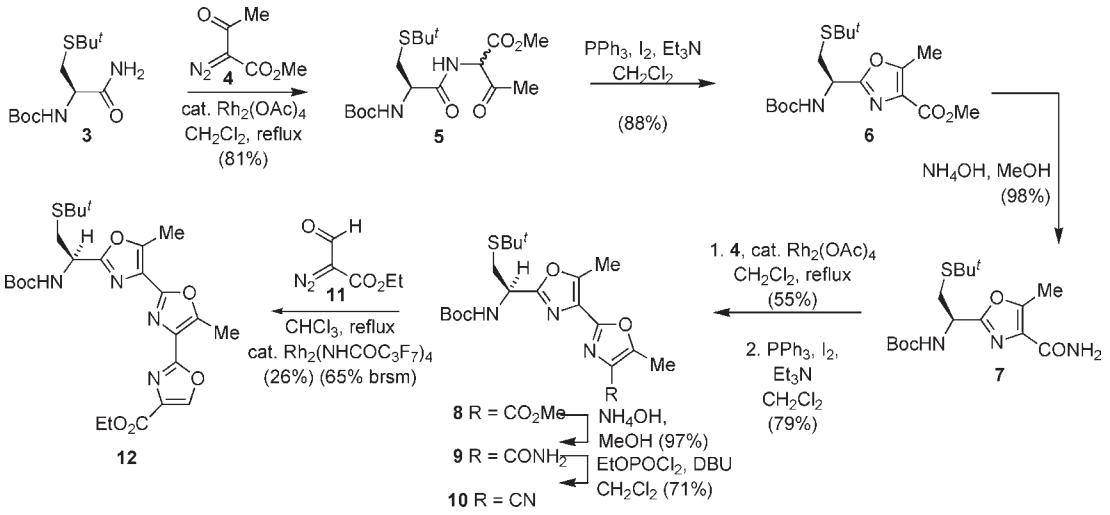

Scheme 4. Synthesis of Left-hand Tris-oxazole Fragment (Rings E−G)

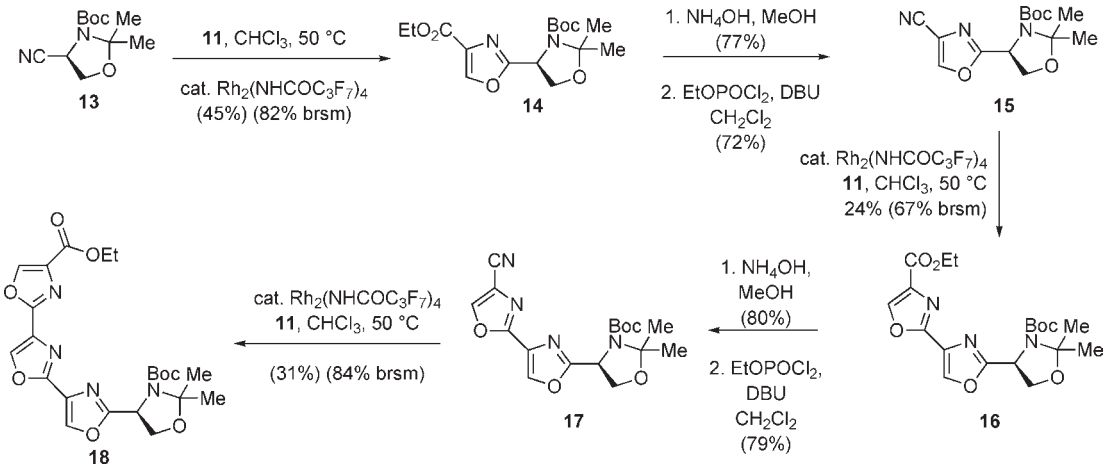

strategic disconnection into two tris-oxazole fragments is the same as the one employed by Doi et al.,[25] the synthesis of the oxazole rings themselves is completely different. Thus, the oxazoles would be constructed using reactive transition-metal carbene intermediates, formed upon treatment of diazocarbonyl compounds with catalytic amounts of dirhodium(II) complexes, to give oxazoles upon reaction with nitriles, or with carboxamides followed by cyclodehydration as outlined in Scheme 2. Although we have employed this tactic in the construction of the oxazole building blocks of other biologically active natural products such as nostocyclamide,[34] diazonamide A,[35,36] promothiocin A,[37] and amythiamicin A,[38] its use for the multiple oxazole rings of telomestatin would constitute a supreme test for the robustness of the methodology.

The synthesis of the right-hand tris-oxazole started with the protected cysteine carboxamide **3** that underwent smooth carbene N−H insertion upon treatment with methyl diazoacetoacetate **4** and dirhodium(II) tetraacetate, added in portions over a 48 h period, to give the ketoamide **5**, as an inconsequential mixture of diastereomers. Cyclodehydration of ketoamide **5** using the triphenylphosphine/iodine/triethylamine protocol[39] delivered the first oxazole **6** in excellent overall yield. Conversion of ester **6** into carboxamide **7** was followed by a second rhodium-catalyzed carbene transformation to give, after cyclodehydration, the bis-oxazole **8** (Scheme 3). Transformation of ester **8** into nitrile **10**, via dehydration of the carboxamide **9**,[40] set the stage for the direct installation of the third oxazole by dirhodium(II)-catalyzed reaction with the formyl diazo compound **11**, although a switch of catalyst to dirhodium tetrakis(heptafluorobutyramide) proved necessary. We had previously found that catalysts with fluorinated carboxamide ligands were superior in other reactions of diazocarbonyl compounds,[41−43] and in this case the use of $Rh_2(NHCOC_3F_7)_4$ was essential for the successful preparation of the desired tris-oxazole **12**, albeit in modest yield (65% based on recovered nitrile starting material). The recovery of unreacted nitrile appears to be a feature when using diazoaldehyde **11** (see also below) and is due to the competing formation of a carbene dimer as previously been noted by others.[44] The dimer is tentatively assigned as ethyl 2-(2-ethoxy-2-oxoethylidene)-1,3-dioxole-4-carboxylate (see Supporting Information), presumably

dx.doi.org/10.1021/ja109158k |J. Am. Chem. Soc. 2011, 133, 1044–1051

formed by Wolff rearrangement followed by 1,3-dipolar cycloaddition of the resulting ketene to another aldehyde carbene.

A trio of dirhodium(II)-catalyzed reactions was also used to access the left-hand tris-oxazole **18** comprising rings E−G. Thus, nitrile **13**, prepared from the serine-derived methyl ester,[45] was directly converted into oxazole **14** by $Rh_2(NHCOC_3F_7)_4$-catalyzed reaction with diazo aldehyde **11** (82% based on recovered nitrile starting material). A second cycle was initiated by conversion of ester **14** into the corresponding carboxamide and hence nitrile **15**, the substrate for a second dirhodium(II)-catalyzed reaction with diazo aldehyde **11**, to give bis-oxazole **16**. Running the reaction sequence for a third time provided the required tris-oxazole **18** (Scheme 4).

Having successfully synthesized both trisoxazoles **12** and **18** employing a total of six dirhodium(II)-catalyzed reactions to form all oxazole rings, it remained to effect the pivotal coupling of the two fragments. The amine of cysteine-based trisoxazole **12** was deprotected using HCl in dioxane, while the serine-based trisoxazole **18** was saponified with lithium hydroxide. For the key amide coupling, several coupling reagents and conditions were investigated, with the combination of *O*-benzotriazol-1-yl-tetramethyluronium hexafluorophosphate (HBTU) and triethylamine giving the best yield of 68% of amide **19**. For the critical macrolactamization step, first the ethyl ester of **19** was hydrolyzed, and this was followed by deprotection of the Boc-amine again using HCl in dioxane. Although several reagents were used to bring about the macrolactamization, the use of HBTU and triethylamine again proved superior, and this delivered the desired macrolactam **20** in 51% yield over three steps. Finally, alcohol **20** was dehydrated with methanesulfonyl chloride and DBU in 58% yield to give alkene **21** (Scheme 5). The spectroscopic properties of macrolactams **20** and **21** are fully in accord with their structure and closely match those reported by Shin-ya and co-workers.[25] Because these researchers have previously converted macrolactam **21** into telomestatin **1**,[25] our successful route to this key intermediate constitutes a formal synthesis of the natural product.

Biophysical Analysis of Ligand−Quadruplex Interactions. The remarkable biological activity of natural telomestatin is well documented and is based on its ability to stabilize G-quadruplex structures.[12] However, the value of chemical synthesis is that it also provides novel compounds, and, having a range of poly oxazoles available, we investigated their binding and stabilizing effects on a human telomeric intramolecular G-quadruplex using a synthetic oligonucleotide sequence 5′-AGGGTTAGGGTTAGGGTTAGGG (*h*-Tel). Far-UV CD spectra were collected on a 4 μM aqueous solution of *h*-Tel, containing 100 mM KCl and 10 mM potassium phosphate buffer at pH 7.0.[46] In the first instance, we examined the effects of compound **22** (as its HCl salt), a tris-oxazole fragment, prepared by the deprotection of compound **12**, and the acyclic hexa-oxazole precursor **19**, the latter to explore the necessity for a rigid cyclized framework to facilitate quadruplex binding. The CD melting curve for *h*-Tel, monitored at 290 nm (Figure 2a), gave a transition midpoint T_m = 69 ± 2 °C; however, we observed no significant changes in the T_m of *h*-Tel in the presence of >4 mol equiv of each of these ligands (ΔT_m < 1 °C). In contrast, the effects on quadruplex stability of binding the macrocyclic hexa-oxazoles **20** and **21** were much more significant. Both ligands produced substantial shifts in the unfolding transition, indicating T_m values >92 °C, and large stabilizing effects on *h*-Tel of >25 °C. Monitoring the intensity of the bands at 265 and 290 nm produces similar T_m values.

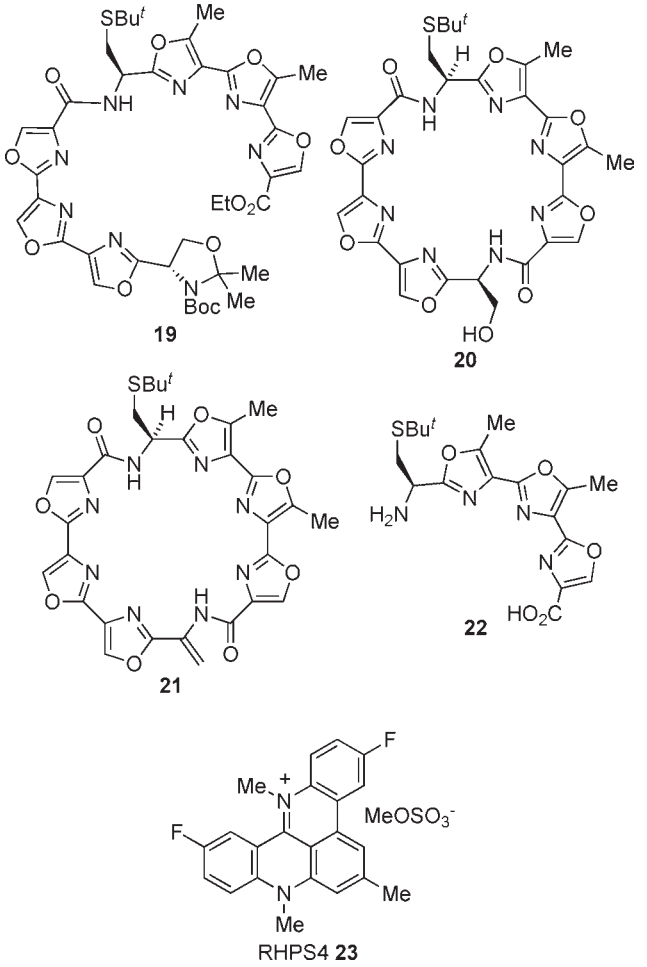

We extended our analysis to ESI-MS studies of the ligand−quadruplex interactions to determine ligand binding stoichiometries using 100 mM ammonium acetate solutions containing 8 μM *h*-Tel and 4−6 μM of ligands **20** and **21**. We could readily detect noncovalent 1:1 and 2:1 ligand complexes in the gas phase for both **20** and **21** (Figure 2b), as seen for other macrocyclic hepta-oxazoles.[17,18] Interestingly, the ligand-free quadruplex and each of the bound complexes revealed a distribution of species with different numbers of bound NH_4^+ ions, as illustrated for **20** in Figure 2c. Three independent analyses of *h*-Tel in the absence of ligands revealed similar distributions with the species with one NH_4^+ ion being the most abundant; however, n = 0, 2, and 3 are also well represented. When we compared the distribution for the unbound *h*-Tel, the 1:1, and 2:1 ligand complexes, there was a clear correlation between the number of bound ligands and the number of bound ammonium ions with a minimum of one cation per ligand. For example, in the 1:1 complex with **20**, species corresponding to 2 and 3 bound NH_4^+ ions are abundant, but for the 2:1 ligand complex, the distribution profile increases by one. These features are also evident in the profile for complexes of **21** (Figure 2d).

To assess whether these trends in the distribution of bound cations are specific to **20** and **21**, or arise from an increase in the structural stability of the complexes, which enhances the retention of tetrad-bound ammonium ions in the gas phase, we carried out studies in parallel with the polycyclic acridinium cation

dx.doi.org/10.1021/ja109158k |*J. Am. Chem. Soc.* 2011, 133, 1044–1051

Scheme 5. Combination of Right-hand Tris-oxazole Fragment (Rings A−C) with Left-hand Tris-oxazole Fragment (Rings E−G), and Macrocyclization − A Formal Total Synthesis of Telomestatin

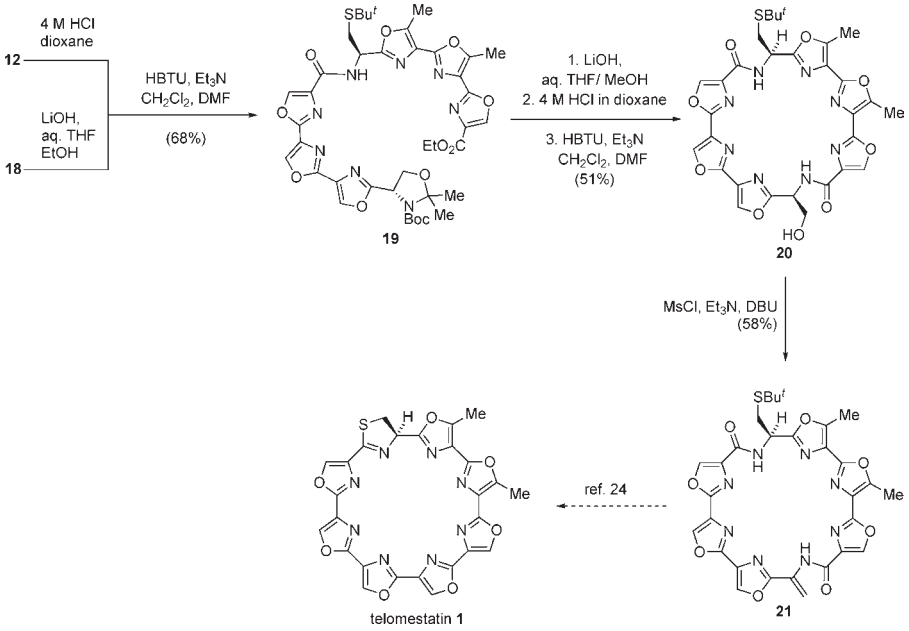

RHPS4 **23**, which is a potent telomerase inhibitor[47,48] with similar quadruplex stabilizing properties.[46] Compound **23** carries a net positive charge delocalized across the acridinium ring system, which enhances stacking on the terminal G-tetrads. Under the same experimental conditions, we were readily able to detect both 1:1 and 2:1 ligand complexes with **23**; however, the distribution of species in terms of the number of bound ammonium ions showed a quite different profile as compared to **20** and **21** (Figure 2d, bottom). The number of bound cations appears to be independent of the number of bound ligands, with the predominant species in both 1:1 and 2:1 complexes showing the binding of only a single cation. Thus, the effects observed for **20** and **21** appear to be ligand-specific and were investigated further in molecular dynamics simulations.

Modeling Cation Involvement in Drug−Quadruplex Interactions. Initially, we performed geometry optimization of the two *seco*-derivatives (**20** and **21**) and showed using DFT calculations that K^+ forms a stable complex in which the oxazole macrocycles are distorted from planarity. Starting structures for ligand−quadruplex modeling were generated by initially screening against a number of rigid tetrad structures, and the models were clustered and ranked by energy. Subsequently, unrestrained molecular dynamics calculations, employing an explicit solvent model (see Supporting Information), were performed for 500−1000 ps at 300 K using the (2 + 2) *h*-Tel antiparallel NMR structure[49] and the X-ray structure of the parallel quadruplex.[50]

On the time scale of the MD simulations (≤1 ns), the 1:1 ligand complex, with three K^+ ions bound (two sandwiched between the three G-tetrads and one within the ligand macrocycle), is quite stable. MD simulations of G-quadruplex structures generally show evidence for buckling of the terminal tetrads, which in this case is entirely compatible with the optimization of π-stacking interactions with the nonplanar geometry of the ligands. The simulations show that the ligands undergo further partial flattening to optimize stacking interactions and reduce steric clashes with the *tert*-butyl-Cys residue. The MD structures are consistent with the ligand-bound K^+ ion being accommodated within the region of high negative charge density generated by the macrocycle and the guanine O6 of the terminal G-tetrad. Thus, the cation coordinated macrocycle forms a highly complementary capping interaction at the end of the quadruplex, as shown for **21** in the complex with the antiparallel structure (Figure 3a). An offset stacking arrangement is observed, which minimizes steric contacts and places the *tert*-butyl-Cys residue in the wider of the four grooves, which is particularly favorable in the context of the antiparallel structure (Figure 3b). Contacts with nucleotides in the diagonal TTA loop form many other complementary ligand interactions (Figure 3c), which are unique to, and appear to preferentially stabilize, the complex with the antiparallel structure. Thus, a combination of the ESI-MS data and MD simulations appears to fully rationalize our observations that the *seco*-derivatives of telomestatin form highly stabilizing interactions with G-quadruplex structures mediated by the ability of the macrocycle to coordinate a monovalent cation.

A number of previous studies have explored macrocyclic hexaoxazole frameworks as potent synthetic telemostatin analogues for targeting of G-quadruplex structures. In particular, HXDV, with Val residues accommodated within the macrocycle, results in a similarly distorted nonplanar concave ring geometry.[17,18] Fluorescence studies show that HXDV binds with high selectivity for quadruplex over duplex structures with large increases in thermal stability, as well as potent inhibitory effects on the growth of lymphoblastoma cells (IC_{50} value of around 0.4 μM). A series of related amine and guanidine derivatives of the same macrocycle were synthesized by Nagasawa et al., and in a subsequent paper these studies were extended to a hepta-oxazole with a single amino acid side chain accommodated within the ring.[20,21] In terms of both their chemical structures and their conformational properties, these molecules closely resemble the *seco*-derivatives described in this study. CD studies were used by Nagasawa et al. to demonstrate the ability of a number of ligands to induce the

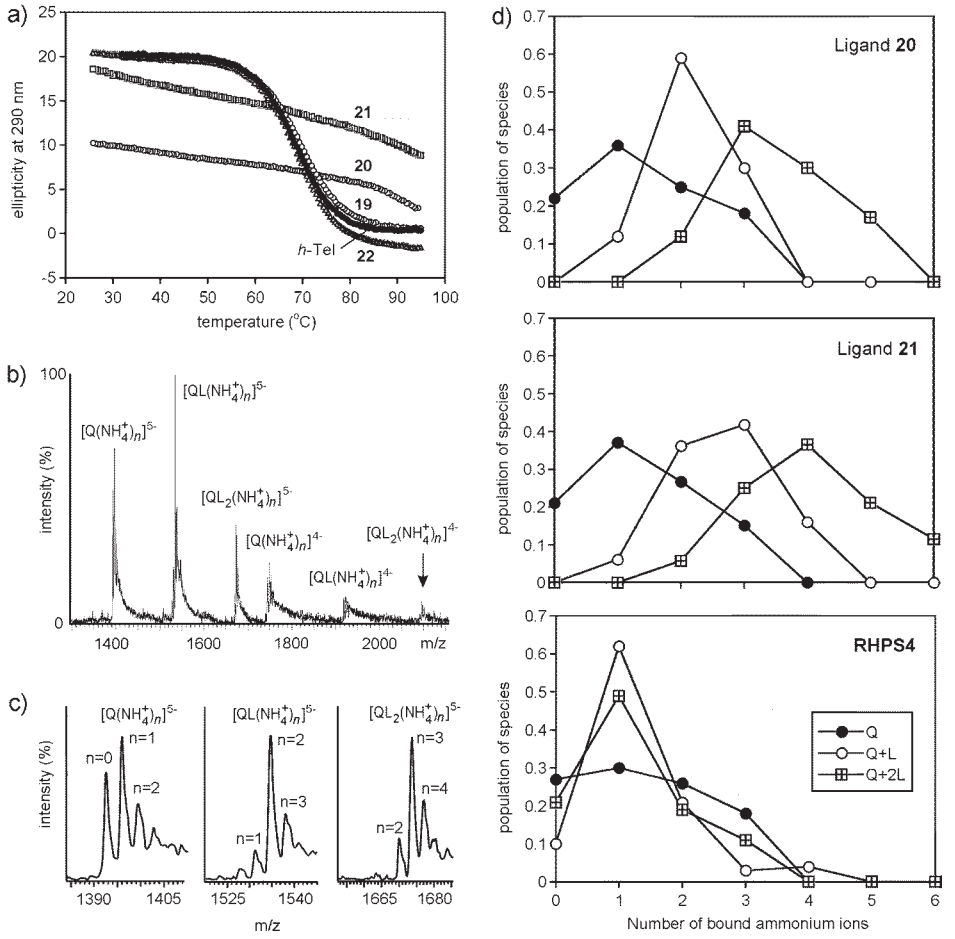

Figure 2. (a) Far-UV CD annealing profiles of *h*-Tel in 110 mM K^+ with 4 equiv of various ligands (**19**, **20**, **21**, and **22**) monitoring the intensity at 290 nm as a function of temperature (*h*-Tel alone shown by the black dots). (b) Representative ESI-MS spectrum of complexes formed between *h*-Tel (Q) and ligand **20** (L), showing the 5- and 4-species observed in the gas phase for Q, QL, and QL_2 with each peak representing a distribution of bound (*n*) ammonium ions. (c) Expansion of peaks for Q, QL, and QL_2 showing the distribution of bound NH_4^+ ions. (d) Normalized distribution of species observed by ESI-MS analysis of *h*-Tel complexes of ligand **20** (top), ligand **21** (middle), and the polyacridinium cation RHPS4 **23** (bottom) in 100 mM ammonium acetate buffer. The sum of the populations for *h*-Tel and for each complex equals one.

folding of telomere-derived DNA sequences, with a preference for stabilizing antiparallel structures. Many of these nonplanar telomestatin analogues showed potent telomerase-inhibitory activity in both cell-free and cell-based assays, and quadruplex-stabilizing properties that were comparable to the natural product. However, the ability of this family of macrocycles to complex monovalent cations, and its importance in forming stabilizing interactions with G-quadruplexes, has remained largely unexplored. A recent MD study on G-quadruplex complexes of telomestatin has noted that K^+ ions were observed to shift from the central cavity between tetrads, or were pulled in from the surrounding solvent, to coordinate with the macrocycle and stabilize the interaction with the terminal G-tetrad.[51]

■ CONCLUSIONS

In this study, the power of rhodium carbene chemistry has been demonstrated in an efficient formal synthesis of the structurally unique natural product telomestatin, in which six oxazole rings are formed using dirhodium(II)-catalyzed reactions of diazocarbonyl compounds. Although the strategic disconnection of the telomestatin macrocycle into two tris-oxazole fragments has precedent in other approaches, the construction of the oxazole rings themselves is completely different. Our approach has allowed access to synthetic oxazoles with different degrees of conformational planarity that bind strongly and stabilize G-quadruplex structures. To rationalize these observations, we present the first experimental evidence from ESI-MS, supported by MD simulations, that the *seco*-derivatives described in this study and by analogy telomestatin recruit metal ions to stabilize the end-capping interaction with a G-tetrad. Despite the distortion of our ligand structures from planarity, cation-mediated interactions and buckling of the G-tetrad produce a highly complementary offset stacking interaction in which the *tert*-butyl-Cys residue is accommodated in the major groove of the antiparallel structure. The potent properties of these and other reported synthetic oxazole offer promise as potential anticancer agents targeted at inhibiting telomerase by stabilizing telomeric G-quadruplexes.

■ EXPERIMENTAL SECTION

General methods, experimental protocols, and spectroscopic characterization data for all compounds are given in the Supporting Information, along with copies of ^1H and ^{13}C NMR spectra. The data for three key compounds are given below. Full details of the CD spectroscopy, ESI mass spectrometry, and the molecular modeling are also given in the Supporting Information.

dx.doi.org/10.1021/ja109158k |*J. Am. Chem. Soc.* 2011, 133, 1044–1051

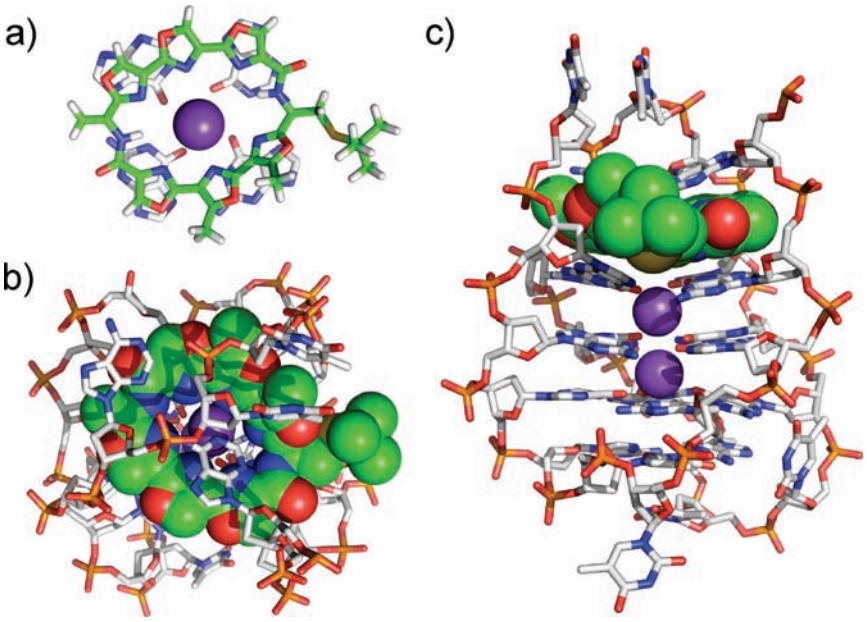

Figure 3. (a) Geometry-optimized structure of **21** (green) showing complexation with K^+ and offset stacking on the terminal G-tetrad of the antiparallel quadruplex; (b) same view from above of the structure of the 1:1 complex of **21** with the antiparallel quadruplex showing the location of the *tert*-butyl-Cys residue in the major groove and the position of the diagonal loop running across the top of the ligand; and (c) same structure viewed from the side showing three bound K^+ ions (including one coordinated between the macrocyclic ring system and terminal G-tetrad) and close contacts with the diagonal loop.

Linear Hexa-oxazole 19. Colorless solid; mp 162−163 °C; $[\alpha]^{D}_{25}$ −21.1 (*c* 0.57, $CHCl_3$); (Found: MNa^+, 885.2885; $C_{40}H_{46}N_8NaO_{12}S$ requires 885.2848); δ_H (270 MHz; 90 °C; DMSO-d_6) 8.89 (1H, s, H-5), 8.83 (1H, s, H-5), 8.79 (1H, s, H-5), 8.71 (1H, s, H-5), 8.66 (1H, d, *J* 8.3, NH), 5.38 (1H, m, NHC<u>H</u>CH$_2$), 5.16 (1H, dd, *J* 6.4, 3.0, NBocC<u>H</u>CHH), 4.35 (2H, q, *J* 7.0, C<u>H</u>$_2$CH$_3$), 4.34−4.29 (1H, m, NBocCHC<u>H</u>H), 4.09 (1H, dd, *J* 9.2, 3.0, NBocCHCCH<u>H</u>), 3.28−3.25 (2H, m, NHCHC<u>H</u>$_2$), 2.74 (3H, s, Me), 2.68 (3H, s, Me), 1.67 (3H, s, Me), 1.55 (3H, s, Me), 1.33 (18H, s, CMe$_3$), 1.33 (3H, t, *J* 7.0, CH$_2$C<u>H</u>$_3$); δ_C (100 MHz; 90 °C; DMSO-d_6) 164.1 (C), 160.8 (C), 160.0 (C), 159.0 (C), 155.5 (C), 155.3 (C), 154.0 (C), 153.8 (C), 150.5 (C), 150.30 (C), 150.27 (C), 144.2 (CH), 142.0 (CH), 140.3 (CH), 140.2 (CH), 136.2 (C), 133.3 (C), 129.7 (C), 128.8 (C), 124.5 (C), 123.7 (C), 93.8 (C), 79.5 (C), 66.4 (CH$_2$), 60.1 (CH$_2$), 54.2 (CH), 47.4 (CH), 42.0 (C), 30.4 (Me), 30.3 (CH$_2$), 27.4 (Me), 20.1 (Me), 20.0 (Me), 13.6 (Me), 10.80 (Me), 10.76 (Me).

Macrolactam 20. Colorless solid; mp >230 °C (lit.,[25] mp not given in literature); $[\alpha]^{25}_{D}$ −4.7 (*c* 0.52, $CHCl_3$) (lit.,[25] $[\alpha]^{25}_{D}$ −6.7 (*c* 0.70, $CHCl_3$)); (Found: MNa^+, 699.1577; $C_{30}H_{28}N_8NaO_9S$ requires 699.1592); δ_H (500 MHz; CD_2Cl_2) 8.57 (1H, d, *J* 6.2, NHC<u>H</u>CH$_2$OH), 8.45 (1H, d, *J* 7.2, NHC<u>H</u>CH$_2$S), 8.33 (1H, s, H-5), 8.30 (1H, s, H-5), 8.28 (1H, s, H-5), 8.25 (1H, s, H-5), 5.50−5.42 (2H, m, 2 × NHC<u>H</u>), 4.20−4.15 (1H, m, C<u>H</u>HOH), 4.03−3.98 (1H, m, CH<u>H</u>OH), 3.26 (1H, dd, *J* 13.2, 5.8, CHC<u>H</u>HS), 3.17 (1H, dd, *J* 13.2, 4.2, CHC<u>H</u>H<u>S</u>), 2.76 (3H, s, Me), 2.71 (3H, s, Me), 1.25 (9H, s, CMe$_3$); δ_C (125 MHz; CD_2Cl_2) 162.6 (C), 161.1 (C), 160.9 (C), 159.4 (C), 156.32 (C), 156.28 (C), 155.4 (C), 154.7 (C), 151.3 (C), 150.8 (C), 140.9 (CH), 140.8 (CH), 140.2 (CH), 138.8 (CH), 136.9 (C), 136.4 (C), 131.0 (C), 129.6 (C), 125.6 (C), 124.6 (C), 65.1 (CH$_2$), 51.5 (CH), 48.2 (CH), 42.5 (C), 32.6 (CH$_2$), 30.6 (Me), 11.7 (2 × Me).

Hexa-oxazole-alkene 21. Colorless solid; mp >230 °C (lit.,[25] mp not given in literature); $[\alpha]^{25}_{D}$ −2.1 (*c* 0.13, $CHCl_3$) (lit.,[25] $[\alpha]^{25}_{D}$ −3.2 (*c* 0.39, $CHCl_3$)); (Found: MNa^+, 681.1484; $C_{30}H_{26}N_8NaO_8S$ requires 681.1487); δ_H (400 MHz; CD_2Cl_2) 9.53 (1H, s, N<u>H</u>CCHH), 8.39 (1H, d, *J* 6.7, N<u>H</u>CH), 8.35 (1H, s, H-5), 8.30 (1H, s, H-5), 8.28 (1H, s, H-5), 8.26 (1H, s, H-5), 6.76 (1H, s, CC<u>H</u>H), 6.76 (1H, s, CCH<u>H</u>), 5.46−5.42 (1H, m, C<u>H</u>CHH), 3.32 (1H, dd, *J* 13.0, 5.7, CHC<u>H</u>H), 3.19 (1H, dd, *J* 13.0, 3.8, CHCH<u>H</u>S), 2.77 (3H, s, Me), 2.72 (3H, s, Me), 1.23 (9H, s, CMe$_3$); δ_C (125 MHz; CD_2Cl_2) 161.4 (C), 159.8 (C), 159.5 (C), 156.7 (C), 156.6 (C), 155.8 (C), 155.1 (C), 152.2 (C), 151.7 (C), 142.0 (C), 141.3 (CH), 140.72 (CH), 140.66 (CH), 139.4 (CH), 137.4 (C), 137.2 (C), 131.3 (C), 130.8 (C), 128.6 (C), 125.9 (C), 124.9 (C), 104.3 (CH$_2$), 48.8 (CH), 43.0 (C), 32.6 (CH$_2$), 31.0 (Me), 12.33 (Me), 12.28 (Me).

■ ASSOCIATED CONTENT

Supporting Information. Full experimental details, copies of ^{1}H and ^{13}C NMR spectra, and details of the CD spectroscopy, ESI mass spectrometry, and molecular modeling. This material is available free of charge via the Internet at http://pubs.acs.org.

■ AUTHOR INFORMATION

Corresponding Author
c.j.moody@nottingham.ac.uk

■ ACKNOWLEDGMENT

We thank the EPSRC and the School of Chemistry at Nottingham for funding. We are grateful to Professor M. F. G. Stevens for providing a sample of RHPS4.

■ REFERENCES

(1) Kelland, L. *Clin. Cancer Res.* **2007,** *13*, 4960–4963.
(2) Hanahan, D.; Weinberg, R. A. *Cell* **2000,** *100*, 57–70.
(3) Neidle, S.; Parkinson, G. *Nat. Rev. Drug Discovery* **2002,** *1*, 383–393.
(4) Searle, M. S.; Balkwill, G. D. In *Quadruplex Nucleic Acids*; Neidle, S., Balasubramanian, S., Eds.; Royal Society of Chemistry: Cambridge, U.K., 2007; pp 131−153.

(5) De Cian, A.; Lacroix, L.; Douarre, C.; Temime-Smaali, N.; Trentesaux, C.; Riou, J. F.; Mergny, J. L. *Biochimie* **2008,** *90*, 131–155.
(6) Rankin, A. M.; Faller, D. V.; Spanjaard, R. A. *Anti-Cancer Drugs* **2008,** *19*, 329–338.
(7) Lingner, J.; Hughes, T. R.; Shevchenko, A.; Mann, M.; Lundblad, V.; Cech, T. R. *Science* **1997,** *276*, 561–567.
(8) Williamson, J. R. *Curr. Opin. Struct. Biol.* **1993,** *3*, 357–362.
(9) Zahler, A. M.; Williamson, J. R.; Cech, T. R.; Prescott, D. M. *Nature* **1991,** *350*, 718–720.
(10) Cragg, G. M.; Grothaus, P. G.; Newman, D. J. *Chem. Rev.* **2009,** *109*, 3012–3043.
(11) Shin-ya, K.; Wierzba, K.; Matsuo, K.; Ohtani, T.; Yamada, Y.; Furihata, K.; Hayakawa, Y.; Seto, H. *J. Am. Chem. Soc.* **2001,** *123*, 1262–1263.
(12) Kim, M. Y.; Vankayalapati, H.; Kazuo, S.; Wierzba, K.; Hurley, L. H. *J. Am. Chem. Soc.* **2002,** *124*, 2098–2099.
(13) Monchaud, D.; Teulade-Fichou, M. P. *Org. Biomol. Chem.* **2008,** *6*, 627–636.
(14) Balasubramanian, S.; Neidle, S. *Curr. Opin. Chem. Biol.* **2009,** *13*, 345–353.
(15) Tsai, Y. C.; Qi, H. Y.; Lin, C. P.; Lin, R. K.; Kerrigan, J. E.; Rzuczek, S. G.; LaVoie, E. J.; Rice, J. E.; Pilch, D. S.; Lyu, Y. L.; Liu, L. F. *J. Biol. Chem.* **2009,** *284*, 22535–22543.
(16) Jantos, K.; Rodriguez, R.; Ladame, S.; Shirude, P. S.; Balasubramanian, S. *J. Am. Chem. Soc.* **2006,** *128*, 13662–13663.
(17) Barbieri, C. M.; Srinivasan, A. R.; Rzuczek, S. G.; Rice, J. E.; LaVoie, E. J.; Pilch, D. S. *Nucleic Acids Res.* **2007,** *35*, 3272–3286.
(18) Rzuczek, S. G.; Pilch, D. S.; LaVoie, E. J.; Rice, J. E. *Bioorg. Med. Chem. Lett.* **2008,** *18*, 913–917.
(19) Pilch, D. S.; Barbieri, C. M.; Rzuczek, S. G.; LaVoie, E. J.; Rice, J. E. *Biochimie* **2008,** *90*, 1233–1249.
(20) Tera, M.; Ishizuka, H.; Takagi, M.; Suganuma, M.; Shin-Ya, K.; Nagasawa, K. *Angew. Chem., Int. Ed.* **2008,** *47*, 5557–5560.
(21) Tera, M.; Iida, K.; Ishizuka, H.; Takagi, M.; Suganuma, M.; Doi, T.; Shin-ya, K.; Nagasawa, K. *ChemBioChem* **2009,** *10*, 431–435.
(22) Iida, K.; Tera, M.; Hirokawa, T.; Shin-ya, K.; Nagasawa, K. *Chem. Commun.* **2009,** 6481–6483.
(23) Rzuczek, S. G.; Pilch, D. S.; Liu, A.; Liu, L.; LaVoie, E. J.; Rice, J. E. *J. Med. Chem.* **2010,** *53*, 3632–3644.
(24) Yamada, S.; Shigeno, K.; Kitagawa, K.; Okajima, S.; Asao, T. Patent EP1350794-A1, 2003.
(25) Doi, T.; Yoshida, M.; Shin-ya, K.; Takahashi, T. *Org. Lett.* **2006,** *8*, 4165–4167.
(26) Yoo, S. *Tetrahedron Lett.* **1992,** *33*, 2159–2162.
(27) Endoh, N.; Tsuboi, K.; Kim, R.; Yonezawa, Y.; Shin, C. *Heterocycles* **2003,** *60*, 1567–1572.
(28) Deeley, J.; Bertram, A.; Pattenden, G. *Org. Biomol. Chem.* **2008,** *6*, 1994–2010.
(29) Atkins, J. M.; Vedejs, E. *Org. Lett.* **2005,** *7*, 3351–3354.
(30) Tera, M.; Sohtome, Y.; Ishizuka, H.; Doi, T.; Takagi, M.; Kazuo, S. Y.; Nagasawa, K. *Heterocycles* **2006,** *69*, 505–514.
(31) Marson, C. M.; Saadi, M. *Org. Biomol. Chem.* **2006,** *4*, 3892–3893.
(32) Flegeau, E. F.; Popkin, M. E.; Greaney, M. F. *Org. Lett.* **2008,** *10*, 2717–2720.
(33) Chattopadhyay, S. K.; Singha, S. K. *Synlett* **2010,** 555–558.
(34) Moody, C. J.; Bagley, M. C. *J. Chem. Soc., Perkin Trans. 1* **1998,** 601–607.
(35) Bagley, M. C.; Hind, S. L.; Moody, C. J. *Tetrahedron Lett.* **2000,** *41*, 6897–6900.
(36) Bagley, M. C.; Moody, C. J.; Pepper, A. G. *Tetrahedron Lett.* **2000,** *41*, 6901–6904.
(37) Bagley, M. C.; Bashford, K. E.; Hesketh, C. L.; Moody, C. J. *J. Am. Chem. Soc.* **2000,** *122*, 3301–3313.
(38) Hughes, R. A.; Thompson, S. P.; Alcaraz, L.; Moody, C. J. *J. Am. Chem. Soc.* **2005,** *127*, 15644–15651.
(39) Wipf, P.; Miller, C. P. *J. Org. Chem.* **1993,** *58*, 3604–3606.
(40) Kuo, C. W.; Zhu, J. L.; Wu, J. D.; Chu, C. M.; Yao, C. F.; Shia, K. S. *J. Chem. Soc., Chem. Commun.* **2007,** 301–303.
(41) Doyle, K. J.; Moody, C. J. *Synthesis* **1994,** 1021–1022.
(42) Cox, G. G.; Miller, D. J.; Moody, C. J.; Sie, E.-R. H. B.; Kulagowski, J. J. *Tetrahedron* **1994,** *50*, 3195–3212.
(43) Brown, D. S.; Elliott, M. C.; Moody, C. J.; Mowlem, T. J.; Marino, J. P.; Padwa, A. *J. Org. Chem.* **1994,** *59*, 2447–2455.
(44) Connell, R. D.; Tebbe, M.; Gangloff, A. R.; Helquist, P.; Åkermark, B. *Tetrahedron* **1993,** *49*, 5445–5459.
(45) Dondoni, A.; Perrone, D. *Org. Synth.* **1999,** *77*, 64–77.
(46) Garner, T. P.; Williams, H. E. L.; Gluszyk, K. I.; Roe, S.; Oldham, N. J.; Stevens, M. F. G.; Moses, J. E.; Searle, M. S. *Org. Biomol. Chem.* **2009,** *7*, 4194–4200.
(47) Gavathiotis, E.; Heald, R. A.; Stevens, M. F. G.; Searle, M. S. *J. Mol. Biol.* **2003,** *334*, 25–36.
(48) Heald, R. A.; Modi, C.; Cookson, J. C.; Hutchinson, I.; Laughton, C. A.; Gowan, S. M.; Kelland, L. R.; Stevens, M. F. G. *J. Med. Chem.* **2002,** *45*, 590–597.
(49) Wang, Y.; Patel, D. J. *Structure* **1993,** *1*, 263–282.
(50) Parkinson, G. N.; Lee, M. P. H.; Neidle, S. *Nature* **2002,** *417*, 876–880.
(51) Agrawal, S.; Ojha, R. P.; Maiti, S. *J. Phys. Chem. B* **2008,** *112*, 6828–6836.